Dielectric Study on the Heterogeneous Dynamics of Miscible Polyisoprene/Poly(vinyl ethylene) Blends: Estimation of the Relevant Length Scales for the Segmental Relaxation Dynamics

Yuji Hirose, Osamu Urakawa,* and Keiichiro Adachi

Department of Macromolecular Science, Graduate School of Science,Osaka University, Toyonaka, Osaka, 560-0043, Japan

Received December 30, 2002

ABSTRACT: Dielectric study was performed on the polyisoprene (PI)/poly(vinyl ethylene) (PVE) miscible blends. We observed the end-to-end vector fluctuation dynamics (normal mode) of PI as well as the two α-relaxation processes corresponding to the segmental motions of PVE and PI. Among these three relaxation modes, the normal mode relaxation behavior was examined in detail. Since this relaxation reflects the dynamics of the length corresponding to the end-to-end distance of PI chain, comparison of the relaxation times for the normal mode and α-processes gives the information about the length scale of the two α-relaxation modes. We estimated the relevant length scales for the segmental motions in the blend and compared them with a single cooperative volume model and a dual length scale model. As a result, the latter model was found to describe better the features of the segmental dynamics in PI/PVE blends.

Introduction

The dynamic properties of polymer blends are a long lasting topic of great interest because of its both their industrial importance and their academic interest. Among a limitless number of polymer blends, miscible blends are the ones in which the component polymers are homogeneously mixed at the molecular level and thus considered as an ideal model system to establish the relationship between rheological properties and blend compositions,so-called blending law.[1] However recent experimental results show that the dynamics of miscible blends is not simple:[2−28] e.g., the time−temperature superposition (tTS) does not hold (thermorheological complexity) in both the flow and transition regions, and broadening of primary relaxation spectrum (α-spectrum) is observed and in some blends two α-peaks appear, so that it is still open to debate about what the causes of such complexity are.

Poly(vinyl ethylene) (PVE)/*cis*-polyisoprene (PI) binary blend is known to be miscible[29−31] and is probably the most extensively studied system over the past decade for the purpose to examine the local dynamical heterogeneity in the miscible state.[4−9,14−16,18−20,22−25] The important factors for the appearance of such heterogeneity are that the component polymers have a large T_g difference (high dynamical asymmetry) and weak interactions between them. As for the dielectric relaxation, measurements not only on PVE/PI blends[6−8,15,23] but also on the diblock copolymer of PVE-*block*-PI[15,23] were already made by several groups. Their findings are summarized below: (1) bimodal loss peaks for the segmental mode appear when the content of PVE is less than 40 wt %, (2) the two peaks are assigned to the segmental motions of PVE (low-frequency peak) and PI (high *f* peak), (3) tTS breaks down in the α-relaxation region, and (4) dielectric relaxation spectra of the diblock copolymer and the blend with the same composition are almost identical. As for the assignment of the observed two loss peaks (point 2), there used to be arguments whether the low T_g component (PI) contributed to both relaxation peaks[7] or only high-frequency peak. However, recent detailed analyses[8,23] have proved that the interpretation of the latter is more reasonable.

Several models have been proposed[9−11,13,18,32,33] to explain such dynamic behaviors in miscible blends since the concentration fluctuation (CF) model was proposed by Zetsche and Fischer.[13,26] The key point of the Zetsche−Fischer model is in the extension of the cooperative volume concept to the binary blend system. It is noted that the segmental motions of two species are assumed to occur in the same single-sized cooperative volume. They utilized the Donth model[34] to predict the relevant length scale of the segmental motion in which the amplitude of the CF was calculated. Chung et al.[18] proposed another essential idea, i.e., the self-concentration (SC), which biases the concentration of one component than average around its segment due to the chain connectivity. On account of the SC effect, each segment experiences the different concentration, therefore this yields two effective glass transition temperatures leading to two separate relaxation times for each component. However, Chung et al. concluded in their paper that their approach (combination of CF and SC) could not describe both the broadening and separation of the component dynamics at the same time. They therefore suggested the necessity of taking into account "inherent dynamic differences" between two components in order to construct more successful models. Since both the concentration bias due to the SC effect and the CF amplitude strongly depend on the size of the volume in which the primary process of the segmental motions takes place, the CF and SC are closely related to each other through the cooperative volume concept and the

* Corresponding author.

10.1021/ma0217940 CCC: $25.00
Published on Web 04/12/2003

important factor for both effects is its volume size.

Kumar et al.[32] added a new idea in the CF model; i.e., the different local concentration should have different volume size because of the difference in T_0 ($=T_g$ − constant) based on the Donth model. Their formulation is derived from the free energy function with the incorporation of the temperature and the composition dependent volume size. To yield two separate relaxation times for each component they also utilized the self-concentration idea. However in their model the size of the volume is relatively large. For example, the relevant size in PI/PVE blends is calculated to be typically 10 nm or more (depending on T) and is much larger than that expected by the original Donth model (1−3 nm at T_g) for single component glasses. Recently, Ediger et al.[20] pointed out the limitation of their theory without considering the intrinsic difference of the component dynamical characters determined by intrachain potentials as suggested by Chung et al.[18] One of the problems in all of the CF models (Zetsche−Fischer, Chung, and Kumar) is in the cooperative volume concept for the binary blend in which a *single sized volume* is adopted; therefore, the characteristic nature of the component species will more or less disappear.

On the other hand, the SC model proposed recently by Lodge and McLeish[33] introduced two *fixed* length scales responsible for the component dynamics. This approach can include the intrinsic difference of the dynamical characters through the two different length scales. They primarily assume that the relevant length scales determining the friction factors of two components will be comparable to the Kuhn lengths of the components. It is widely believed that the length scale on which dynamic glass transition takes place is a temperature-dependent quantity.[35] Although they neglected such T dependence, their model was shown to be able to predict the essential features of the dynamics for miscible blends. Besides this issue, at present no conclusion has yet been reached whether a single length or two different lengths are responsible for the segmental relaxation of binary polymer blends.

In this study, we reexamined the dielectric behavior of PI/PVE blend focusing our attention on the end-to-end relaxation mode (normal mode) of PI. It is well-known that PI has a type-A dipole, and thus the end-to-end vector fluctuation is dielectrically active.[36] In other words, we have a *measure* of the fixed length scale corresponding to the end-to-end distance of a chain to examine the mobility in the blend. This enables us to obtain the information about the length scales of the segments by varying the molecular weight of PI (M_{PI}) and searching for the M_{PI} at which the normal mode peak of PI and segmental mode peak coincide. The goal of our study is to experimentally estimate the relevant length scale for the α-relaxation dynamics in the blend because this kind of information is lacking. Furthermore, the CF models require large cooperative length (the Zetsche−Fischer model requires a 2−7 nm length to reproduce the dielectric data of polystyrene/poly(vinyl methyl ether) blend,[13] and Kumar's model, as mentioned above, also requires a large size for PI/PVE blend[23,32]); therefore, we think the experimental estimation of the cooperative length scale for the widely studied blend system PI/PVE should be necessary to shed light on such the complicated situation. In the first part of this paper, we present the dielectric data including the normal mode relaxation of PI in the blend. Those results are compared with some reported data. In the latter part of the paper, the relevant length scales for the segmental dynamics are discussed.

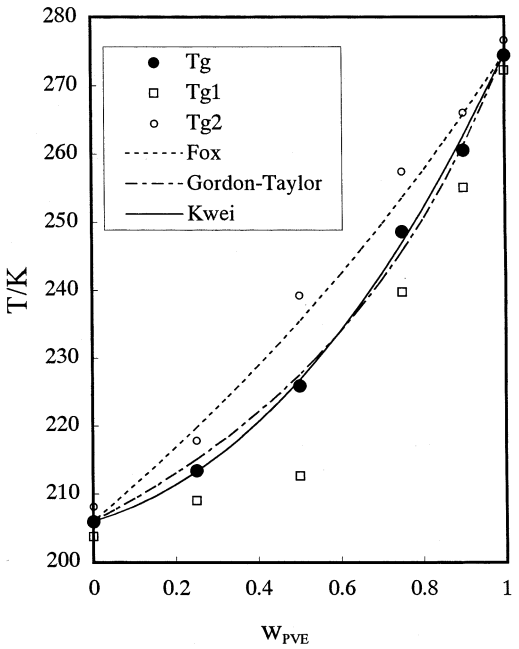

Figure 1. Dependence of T_g on the PVE weight fraction for PI-115/PVE-602 blends. T_{g1} and T_{g2} are the beginning and ending temperatures of the glass transition.

Table 1. Characteristics of PI and PVE Samples

			microstructure/%		
code	$10^{-3}\,M_w$	M_w/M_n	*cis*-1,4	*trans*-1,4	vinyl
PI-17	1.7	1.08	62	32	6
PI-38	3.8	1.05	67	27	6
PI-115	11.5	1.06			
PVE−602	60.2	1.01	1	1	98

Experimental Section

All samples used in this study were prepared by anionic polymerization using *sec*-butyllithium as an initiator and *n*-heptane as a solvent at room temperature. To prepare PVE, 1,3-butadiene was polymerized by using dipiperidinoethane as a modifier[37] at 0 °C. The microstructure of the samples was determined by ^{1}H NMR and ^{13}C NMR (JNM-LA500). Weight-average molecular weight (M_w) of PI-115 and PVE−602, and polydispersity index (M_w/M_n) of all samples were determined by a gel permeation chromatograph, GPC, equipped with a light scattering detector (Tosoh LS 8000). Number-average molecular weights (M_n) of PI-17 and PI-38 were determined by an end group analysis with ^{1}H NMR and converted to M_w using M_w/M_n values which were determined from a GPC calibration curve. Sample characteristics are shown in Table 1.

Glass transition temperature T_g was measured by a differential scanning calorimeter (DSC-20, Seiko Instruments & Electronics Ltd.) at a heating rate of 10 K/min. T_g was determined as the middle point of the transition. For dielectric measurement, capacitance bridge (General Radio 1615A) was used. The frequency range was from 20 Hz to 100 kHz.

Results and Discussion

I. Glass Transition Temperature. Figure 1 shows the dependence of T_g for PI-115/PVE-602 blends on the weight fraction of PVE (w_{PVE}). In this figure, the beginning and ending temperatures of the glass transition, denoted as T_{g1} and T_{g2}, respectively, are also plotted.

It can be seen that $T_g(w_{PVE})$ shows a negative deviation from a linear relationship and the width of the transition ($T_{g1} - T_{g2}$) is much wider than that for the pure component. The broadening of the transition has been considered to be a consequence of at least two factors, i.e., composition fluctuation (CF) and the self-concentration (SC) effects. $T_g(w_{PVE})$ data are compared with three equations: the Fox (eq 1),[38] Gordon−Taylor (eq 2),[39] and Kwei (eq 3)[40] equations.

$$\frac{1}{T_g} = \frac{w_{PVE}}{T_g^{PVE}} + \frac{1 - w_{PVE}}{T_g^{PI}} \quad (1)$$

$$T_g = \frac{(1 - w_{PVE})T_g^{PI} + k_{GT}w_{PVE}T_g^{PVE}}{(1 - w_{PVE}) + k_{GT}w_{PVE}} \quad (2)$$

$$T_g = \frac{(1 - w_{PVE})T_g^{PI} + k_K w_{PVE}T_g^{PVE}}{(1 - w_{PVE}) + k_K w_{PVE}} + qw_{PVE}(1 - w_{PVE}) \quad (3)$$

where T_g^{PVE} and T_g^{PI} stand for the glass transition temperatures of the pure PVE and PI, respectively, and k_{GT}, k_K, and q are the experimental fitting parameters. While eq 1 has no fitting parameter, eqs 2 and 3 contain one and two parameters, respectively. We fit the experimental data to eqs 2 and 3 by using a nonlinear least-squares method. The values of the parameters were found to be $k_{GT} = 0.458$, $k_K = 0.735$, and $q = -33.2$ K.

As is seen in Figure 1, eq 1 apparently fails to reproduce the data as indicated by Chung et al.[18] Roovers and Toporowski[3] reported that $T_g(w_{PVE})$ did not follow the eq 2 and a systematic increase of the parameter k_{GT} (from $k_{GT} = 0.20$ to 0.74) with decreasing w_{PVE} appeared. By closely looking at our result, the T_g data deviate from the dash−dotted line (eq 2) negatively at low w_{PVE} and positively at high w_{PVE} indicating a trend similar to their result. Furthermore, the k_{GT} value we obtained is nearly the average value of their reported values. Therefore, our data are consistent with theirs. On the other hand, eq 3 is found to describe the T_g data best as is seen in the figure. For the data analysis discussed later, we use eq 3 to represent the blend T_g.

II. Composition Dependence of Normal Mode Process in the Blend. Figure 2 shows the master curves of ϵ'' for the normal mode process of PI-115 in the blends with PVE-602. Here the reference temperature T_s is 333 K. The time−temperature superposition (tTS) principle approximately holds except for the frequency regions higher than the normal mode peak for all blends. To compare relaxation time (τ) distribution, the shape of $\epsilon''(f)$ for pure PI is shown in the figures by solid lines. As seen in these figures, there is no difference for the shape among all compositions indicating that the normal mode process is thermorheologically simple in the temperature and frequency ranges examined here. As is well-known, the normal mode reflects the whole chain motion so that the spatial and/or time averaging effect over the heterogeneous environment due to its large size might play a role here. This effect will lead to the simple dynamical behavior as observed here.

The relaxation strength $\Delta\epsilon$ of the normal mode for PI-115/PVE-602 blends is plotted against the weight fraction of PI in Figure 3. The normal mode intensity $\Delta\epsilon$ is written as[36]

$$\Delta\epsilon \propto \rho_{blend}(1 - w_{PVE})F\frac{\langle r^2\rangle}{M_{PI}} \quad (4)$$

Here ρ_{blend} is the density of the blend, F the ratio of the internal to external electric field, $\langle r^2\rangle$ the end-to-end distance, and M_{PI} the molecular weight of PI. Assume that the change in ρ_{blend} and F with the blend composition is negligible; the proportionality of $\Delta\epsilon$ with respect to $1 - w_{PVE}$ observed here suggests that the chain dimension of PI does not change upon blending PVE. This result is reasonable considering that no specific interaction between PI and PVE exists.[31]

III. Composition Dependence of Segmental Mode Process in the Blend. Figure 4 shows the master curves of ϵ'' for PI-115/PVE-602 blends in the α-relaxation regions. Here we took 243 K as T_s. The segmental peaks become bimodal in the range of the PVE content less than 35 wt %. This behavior is in harmony with the data of Alegria et al.[6] They reported that the blend with PVE composition less than 40 wt % exhibit two separate α-peaks. These two peaks have already been analyzed in detail and ascribed to the segmental motions of PVE (low f peak) and PI (high f peak), respectively.[8,23] Here we refer to these two peaks as peak I (low f) and peak II (high f).

The time−temperature superposition (tTS) principle apparently breaks down in the range of frequency from high-frequency side of the normal mode to the low-frequency side of peak I and the ϵ'' curve becomes brader as the decrease of temperature. Since the molecular weight (MW) of PI used here is relatively low (for example compared to that in ref 6), high overlapping between the normal mode and peak I is expected. Therefore, one possible origin for the observed breakdown of tTS is that the degree of the overlapping between the normal mode and the peak I will change with T due to the difference in the T dependences of these two modes. (This different T dependence will be discussed in the next section.) To eliminate this factor, we subtracted the contribution of the normal mode from the loss curves at various temperatures in Figure 5. To do this, the relaxation time of the normal mode peak was estimated by extrapolation using the WLF equation. In this figure, it can be seen that the tTS approximately holds for PVE 25 wt %. The shape of ϵ'' is the same with that of pure PVE as shown by the solid curve, and the change of T does not alter the shape so much. Therefore, the break down of tTS in PVE25% blend (shown in Figure 4c) is mainly due to the overlapping effect, i.e., the different T dependences between the normal mode of PI and segmental mode of PVE (peak I). On the other hand, in the PVE 75 wt % blend, the shape of ϵ'' is apparently broader than that of pure PVE and it changes with temperature (breaking down of tTS) as shown in Figure 5b. The degree of broadening observed in the PVE 75% blend is almost the same with that reported by Alegria et al.[6] in which high MW PI was used thus the overlapping effect was negligible. This broadening of ϵ'' curves observed in PVE 75% is considered to be a consequence of the concentration fluctuation (CF) effect.

IV. Effective Glass Transition Temperature for Each Component in the Blend. Temperature dependence of the normal mode relaxation time τ_n for PI in all blends are shown in Figure 6a. Assuming that the

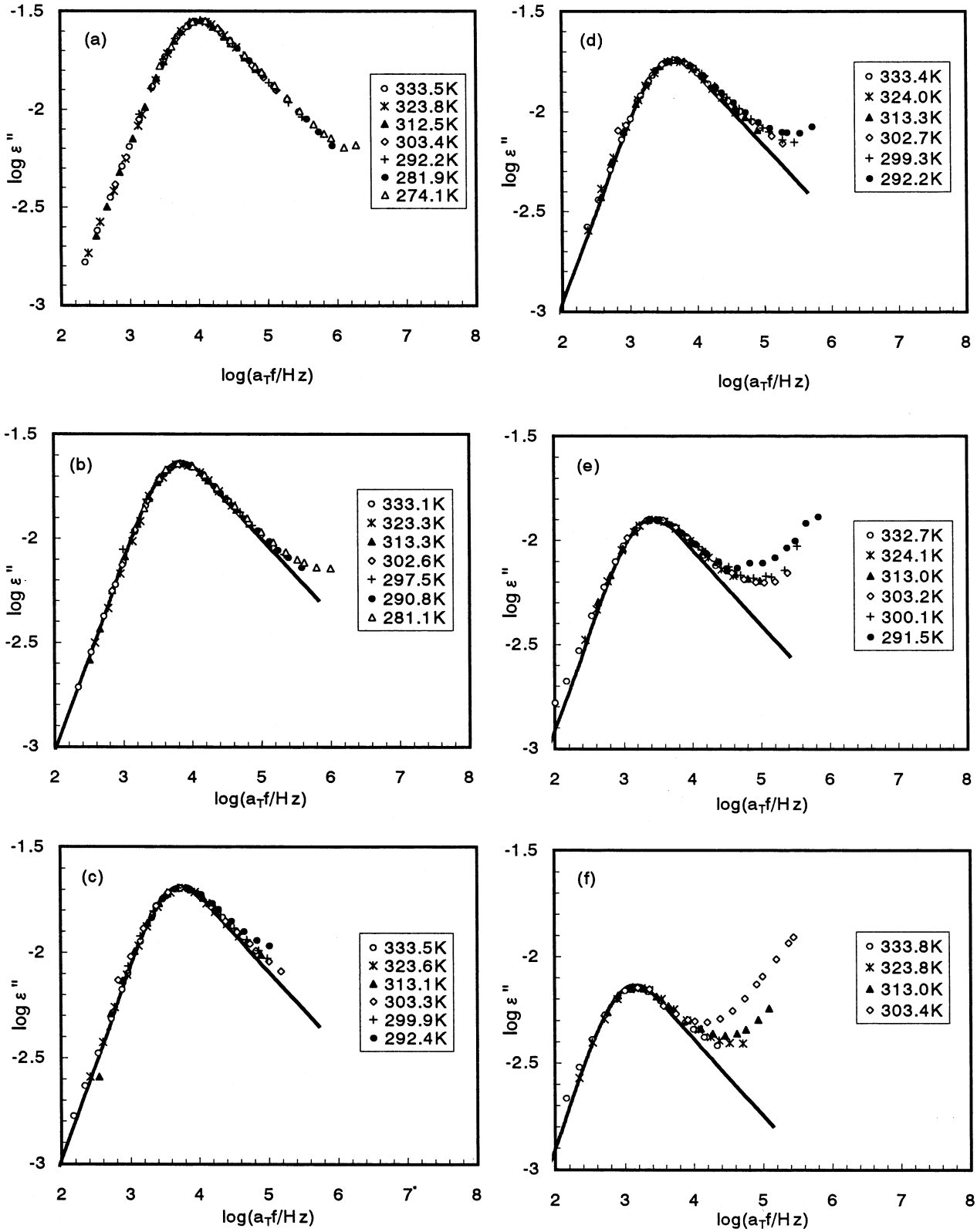

Figure 2. Master curves of ϵ'' for PI-115/PVE-602 blends ($T_s = 333$ K): (a) neat PI; (b) PVE 15 wt %; (c) PVE25 wt %; (d) PVE35 wt %; (e) PVE54 wt %; (f) PVE75 wt %. The solid lines represent the shape of ϵ'' curve of pure PI-115.

functional forms of $\tau_n(T)$ are the same for all the blend compositions, we superposed τ_n data of the blends to that of pure PI by the horizontal shift through changing the reference temperature $T_s(w_{PVE})$ and the result is shown in Figure 6b. Here T_s of pure PI, $T_s(0)$, was chosen to be 333 K.

In these figures, the solid lines are the WLF equation represented by

$$\log \tau_n - \log \tau_{n,s}(\equiv \log a_T) = -c_1(T - T_s)/(c_2 + T - T_s) \quad (5)$$

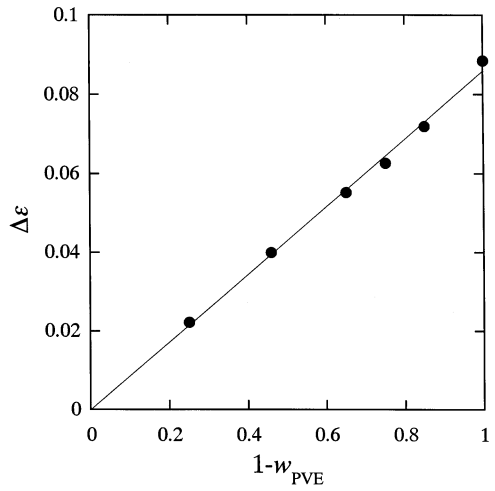

Figure 3. Composition dependence of the normal mode relaxation strength ($\Delta\epsilon$) for PI-115/PVE-602 blends.

where c_1, c_2, and log $\tau_{n,s}$ are the constants.[41] These constant values were determined to be 4.09, 185.5 K, and −4.77, respectively. From the determined $T_s(w_{PVE})$, the effective glass transition temperature $T_g^{eff}(w_{PVE})$ for the whole chain dynamics of PI in the blend can be estimated by the following equation.

$$T_g^{eff}(w_{PVE}) = T_s(w_{PVE}) - [T_s(0) - T_g^{PI}] \qquad (6)$$

It should be noted here that, according to ref 3, PI and PVE homopolymers have slightly different c_1 and c_2 values, indicating that the procedure we adopted here to deduce T_g^{eff} is not correct in a strict sense. However, even if we used different sets of WLF parameters which correspond to those for pure components (in ref 3), the error in the determination of T_g was found to be less than 3 K. Therefore, this method will yield at most 3 K error in the T_g^{eff} estimation for PI/PVE blends. On the other hand, it is also known that the normal mode and segmental mode have slightly different T dependences around T_g.[42,43] However we could not detect such small differences in the obtained data for pure PI and found that the normal and the segmental mode shift factors could be represented by a single set of the WLF parameters. Therefore, the determined T_g^{eff} of PI reflects an average value for both molecular motions.[44]

By using the segmental mode shift factors of the blends, a similar procedure is applicable in principle. However two or three peaks overlap in α-relaxation region, and tTS does not hold as shown in Figure 4; thus, the determination of the accurate shift factors over a wide T range was difficult. Because of this, we limited this procedure to the peak I (PVE segmental mode) for the blend of w_{PVE} higher than 0.54 including pure PVE and the temperature dependencies of the maximum frequency were used to determine T_g^{eff} of the segmental motions of PVE.

It should be mentioned that T_g^{eff} values of two components were determined from different dynamical modes (normal mode for PI and segmental mode for PVE) and thus the temperature range in which we deduced the shift factors are different: that of PI was determined at temperatures from T_g + 60 K to T_g + 120 K while that of PVE was determined in the range from T_g + 10 K to T_g + 40 K. Therefore, there is a possibility that some systematic error is incorporated differently in the two T_g^{eff} data. However, we ruled out this possibility from the reason described above; i.e., the shift factors of normal mode and segmental mode of PI could be approximately regarded as the same.

Two sets of T_g^{eff} thus determined are compared with DSC T_g in Figure 7 along with the literature data,[19] which were determined by NMR measurement. Since there exists slight discrepancy in the values of T_g of pure components between ours and literature data,[19] e.g., the difference in T_g of PI ($\Delta_{PI} = T_g$(this study) − T_g(ref 19)) is −5 K and that of PVE (Δ_{PVE}) is +3 K, we corrected NMR data by adding the factor of $\Delta = (\Delta_{PI} - \Delta_{PVE})w_{PVE} - \Delta_{PI}$. This comparison clearly shows that T_g^{eff}'s of PI and PVE are different from the DSC T_g and exhibit almost the same behavior as the NMR data.

The SC theory by Lodge and McLeish[33] assumes that the T_g^{eff} of component A in an A/B mixture is determined by the local concentration of A in the volume relevant to the segmental motion. Inside the volume the concentration of A is biased due to the chain connectivity. In their theory the local concentration (volume fraction) of A denoted as ϕ_{eff} is expressed by

$$\phi_{eff} = \phi_s + (1 - \phi_s)\phi \qquad (7)$$

where ϕ_s and ϕ are the "self-concentration" and average concentration corresponding to the component A, respectively. T_g^{eff} corresponds to the T_g at $\phi = \phi_{eff}$ and two components possess their own T_g^{eff} in the blend. They assumed that the size of the local volume should be comparable to the cube of the Kuhn length l_K and ϕ_s is determined as

$$\phi_s = C_\infty M_0/k\rho N_{AV}V \qquad (8)$$

where C_∞ is the characteristic ratio (defined as $C_\infty \equiv l_K/l$, where l is the bond length), M_0 is the repeat unit molar mass, k is the number of backbone bonds per monomeric unit, N_{AV} is the Avogadro number, ρ is the density, and V is equal to l_K^3. The calculated T_g^{eff} for PI and PVE by using the parameter in ref 33 ($l_K^{PI} = 0.68$ nm, $l_K^{PVE} = 1.16$ nm) are compared with the data in Figure 7. (In this calculation $w_{PVE} \sim \phi_{PVE}$ was assumed.) As already pointed out by Lodge, this model well predicts the T_g^{eff} of PVE but fails for that of PI. Two possibilities are considered here: (1) the reported Kuhn length of PI is too small, and therefore the self-concentration becomes large ($\phi_s = 0.45$), or (2) the relevant length scale will become larger than the l_K of PI by blending PVE. Under such speculation, we regarded ϕ_s as an adjustable parameter used to fit the T_g^{eff} data of PI. The result is shown by the thin solid line in the figure. The value of ϕ_s used here was 0.08 and the corresponding Kuhn length becomes 1.2 nm. This value is comparable to that of PVE (1.16 nm). This means that the relevant length scales for PI and PVE are similar and the idea of single cooperative volume seems to be appropriate. However there is another possibility that this model cannot express the T_g^{eff} correctly. In the following section (section V), we experimentally determine these length scales based on a more direct way and discuss this point in the last section (section VI).

V. Estimation of Relevant Length Scales for Segmental Dynamics in the Blend. Figure 8 shows the master curves of ϵ'' for PI/PVE (75/25) blends composed of PIs with three different molecular weights. Here the reference temperatures were chosen to be 253.5 K for PI-115/PVE-602, 248 K for PI-38/PVE-602,

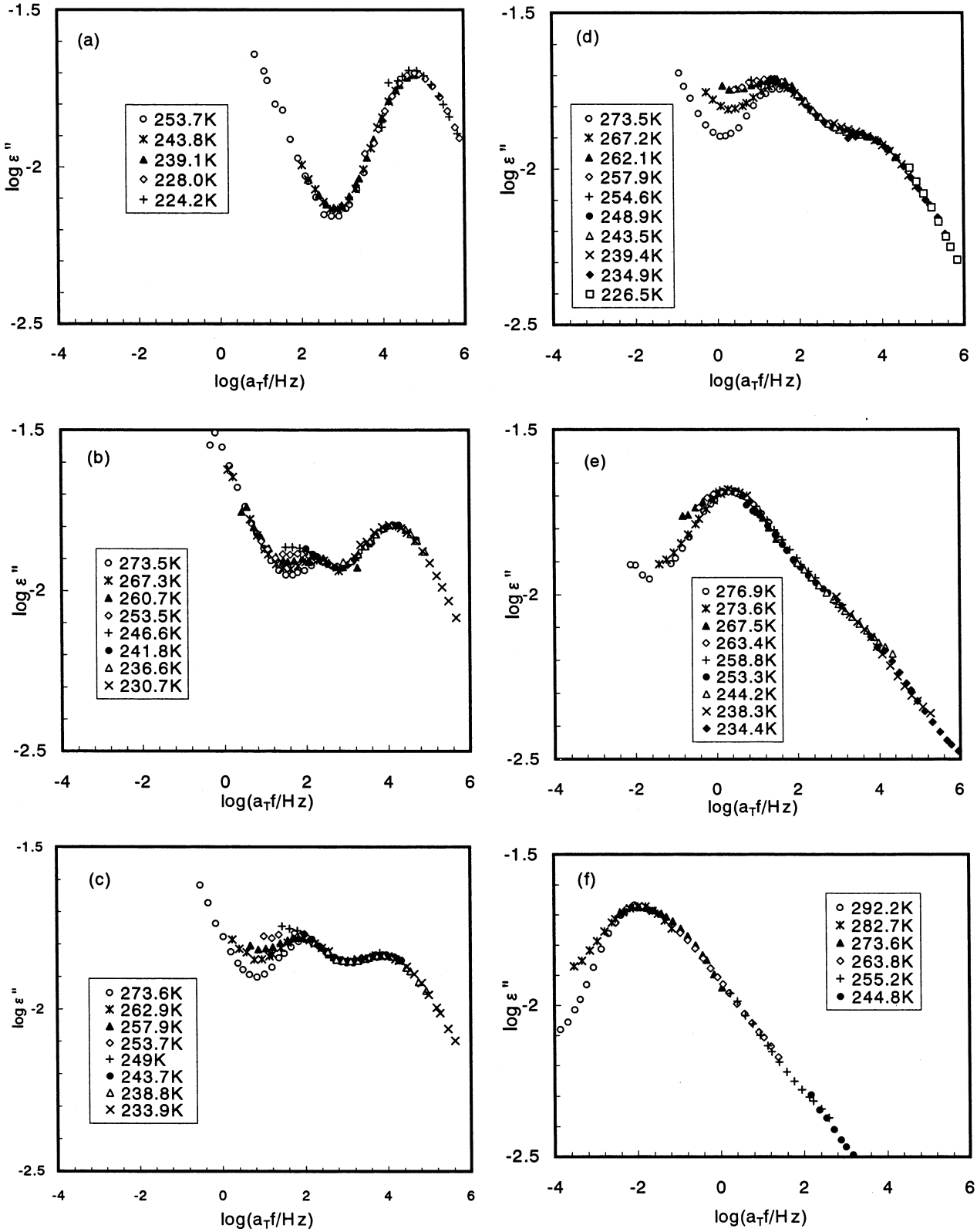

Figure 4. Master curves of ϵ'' for PI-115/PVE-602 blends ($T_s = 243$ K): (a) neat PI; (b) PVE 15 wt %; (c) PVE25 wt %; (d) PVE35 wt %; (e) PVE54 wt %; (f) PVE75 wt %.

and 243 K for PI-17/PVE-602 in order to compare the data at the isofrictional state because the decrease in T_g due to the chain end free volume effect appeared for PI-17 and PI-38 systems. These T_s values correspond to $T = T_g + 40$ K and were determined from the shift factors (a_T) reflecting the PI component dynamics by conforming a_T to a single universal WLF curve. For PI-17/PVE and PI-38/PVE blends the observed ϵ'' are dominated by the response from PI component; therefore, the shift factors almost reflect the temperature dependence of the friction for the PI chain. On the other hand for the PI-115/PVE blend the segmental peak of PVE appears separately between the normal mode and segmental mode peaks of PI. The shift factor of PVE

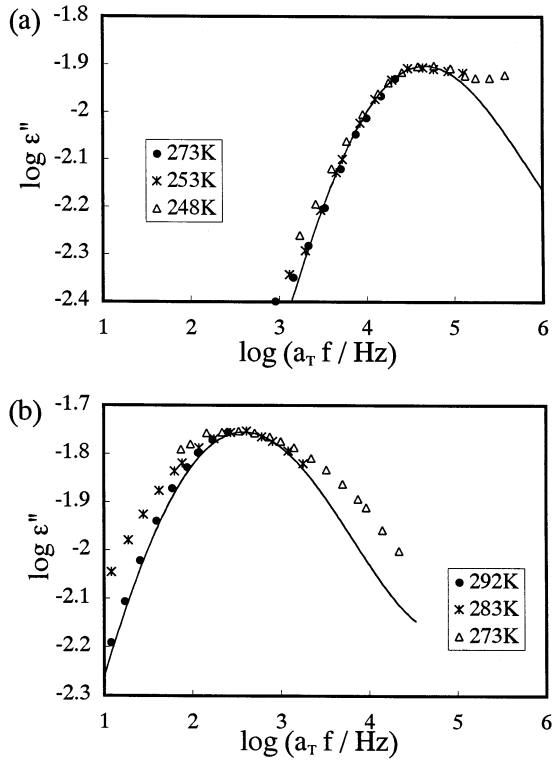

Figure 5. Master curves of ϵ'' for peak I of PVE-602/PI-115 blends after subtraction of the normal mode contribution (Ts = 273 K): (a) PVE25 wt %; (b) PVE75 wt %. The solid lines indicate the data of neat PVE-602.

component is different from that of PI, therefore it was necessary to remove the contribution of PVE component in a_T. Specifically, for the determination of a_T, we used ϵ'' data of PI-115/PVE blend measured at temperatures below 253.5 K, where the segmental mode of PI appeared. It is noted that all the ϵ'' curves merge into a single curve at higher frequency than peak II (segmental mode of PI), indicating the validity of the T_s values adopted here.

As mentioned above, the tTS does not hold especially in the region between the normal mode and peak I. Nevertheless, the master curves presented here are useful for looking at the behavior ranging over the regimes of the segmental and the normal modes. The normal mode peak shifts to the higher f with decreasing M_{PI} while the peaks I and II, which are clearly observable only in the PI-115/ PVE-602 blend, do not change their location. From this figure, it is found that for the PI-17/PVE-602 blend the positions of the normal mode peak and peak I (α-peak of PVE) almost overlap. This means that end-to-end fluctuation of PI and the segmental motion of PVE occur at the similar rate. For more quantitative comparison, Figure 8b shows the ϵ'' data measured at single temperature $T = T_s$ ($=T_g + 40$ K). As is seen in the figure, the peak frequency of the normal mode of PI-17 locates at slightly lower f than the segmental peak of PVE observed in PI-115/PVE-602 blend. The difference is small enough to accurately estimate the molecular weight of PI having the normal mode relaxation time τ_n^{PI} being exactly the same as that of the segmental mode of PVE (τ_s^{PVE}). The extrapolation of τ_n^{PI} to τ_s^{PVE} is shown in Figure 9. Here we assumed the Rouse dynamics ($\tau \sim M^2$) for the nonentangled low MW polymers (PI-17 and PI-38) and drew the line of the slope 2 between these two data. Thus, the obtained

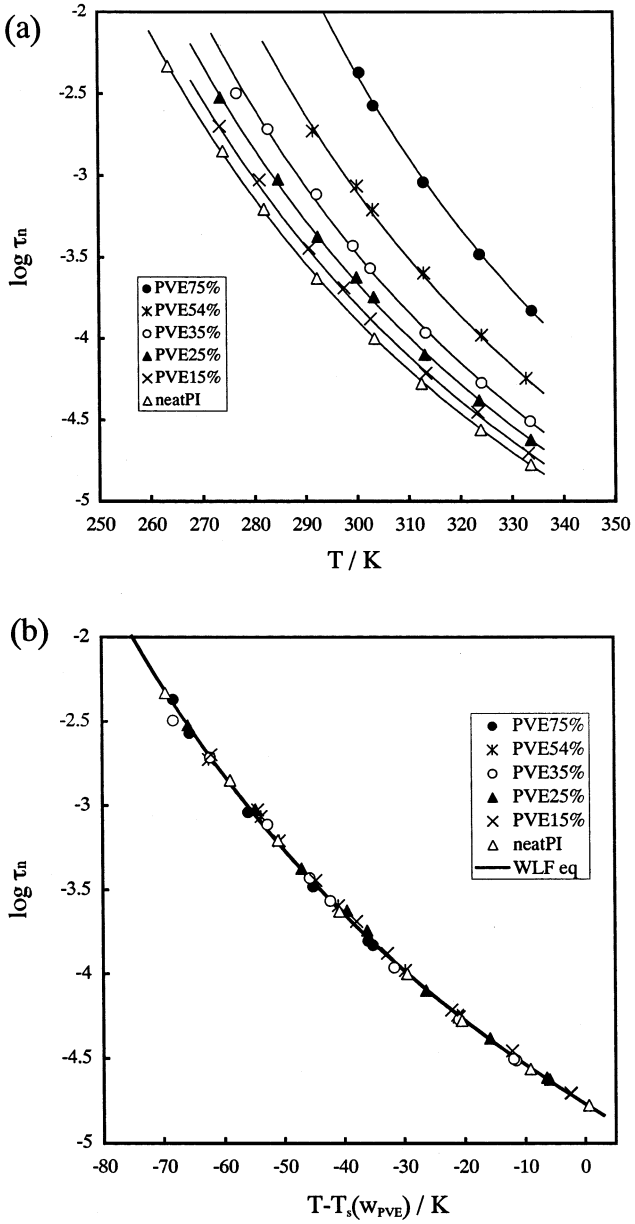

Figure 6. (a) Temperature dependence of the normal mode relaxation times $\tau_n(w_{PVE})$ of PI-115 in the blend with PVE-602. (b) Universal curves of $\tau_n(w_{PVE})$ constructed by varying the reference temperature $T_s(w_{PVE})$ (horizontal shift of τ_n). Here we let $T_s(0)$ be 333 K. The solid lines in parts a and b are the WLF function represented by eq 5 with $c_1 = 4.09$, $c_2 = 185.5$ K, and $\log(\tau_{ns}/s) = -4.77$.

M_{PI} was 1.2×10^3 g mol^{-1}, and the corresponding end-to-end distance r was calculated to be 3.0 nm. Here this length is referred to as r_{long}. For the calculation of r, the following equation reported in ref 45 was used.

$$\log(\langle r^2\rangle/\mathrm{cm}^2) = \log M_w - 16.14 \qquad (9)$$

The same analysis is applicable to the segmental mode of PI. Of course in this case, such an estimation becomes more ambiguous because of the necessity of large extrapolation to low MW region. The assumptions of the Rouse dynamics and Gaussian chain ($\langle r^2\rangle \propto M$) are also not certain. Despite these difficulties, we estimated the M_{PI} in the same way. Errors included in this procedure are discussed in the following section. The τ_s^{PI} value and this extrapolation are also shown in Figure 9. From this,

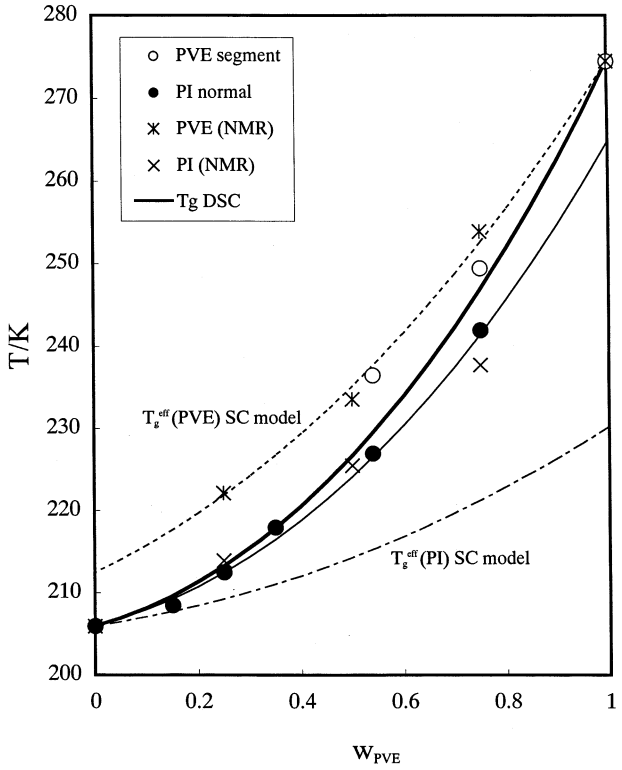

Figure 7. Concentration dependence of the effective glass transition temperatures for the normal mode dynamics of PI and segmental mode of PVE. For comparison the NMR data in ref 19 are shown here. The dashed line and dash−dotted line show the prediction of the original Lodge and McLeish model. Thin solid line is the best fit result of the theory in which the self-concentration of PI was changed as a parameter ($\phi_s = 0.08$ and $l_K^{PI} = 1.2$ nm).

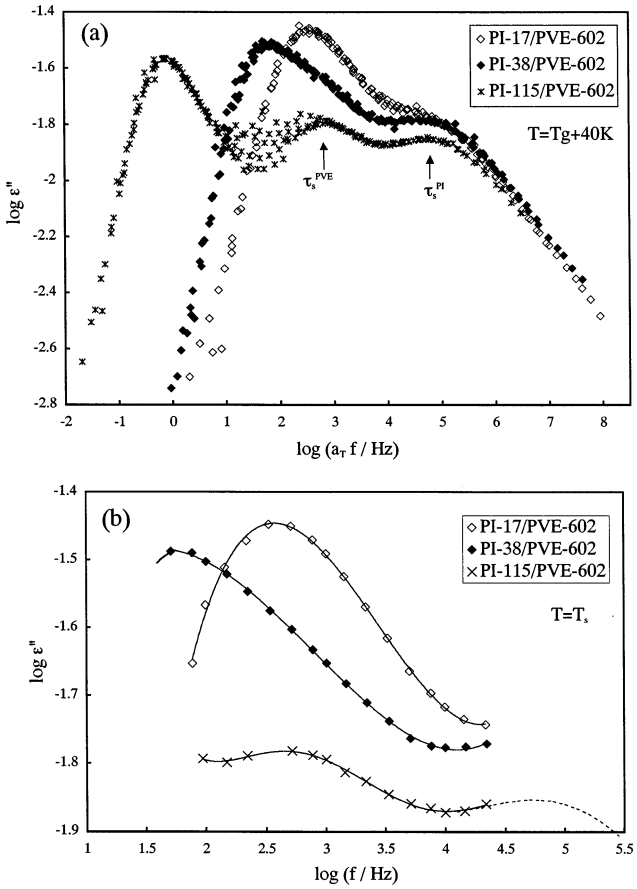

Figure 8. Master curves of ϵ'' for three PI/PVE (75/25) blends with different M_{PI} at $T = T_s$ ($=T_g + 40$ K) (a) and the single temperature data of ϵ'' for the same blends at $T = T_s$ (b).

we obtained $M_{PI} = 1.1 \times 10^2$ g mol^{-1} and $r = 0.9$ nm. Here we refer to this length as r_{short}.

As the first approximation, the segment sizes of PVE and PI are considered to be r_{long} and r_{short}, respectively. However this is a rough approximation because the friction factors of PI and PVE are different even in the homogeneously mixed state. Generally the higher T_g component (PVE) has a higher friction coefficient than the average in the blend and vice versa, for example, by considering the self-concentration effect.[33] Therefore, r_{long} will be larger than the segment size of PVE because the friction coefficient for τ_n^{PI} must be smaller than that for τ_s^{PVE}. On the other hand the friction factors for τ_n^{PI} and τ_s^{PI} are expected to be approximately the same so that the determined r_{short} can be regarded as the segment size of PI. To determine the size of the PVE segment, we corrected the τ_n^{PI} value to have the same friction factor as τ_s^{PVE}. This was made by using both T_g^{eff} data and the WLF equation. From Figure 7, the difference in T_g^{eff} between PI and PVE is found to be 9.4 K for the PI/PVE 75/25 blend and the corresponding shift in the relaxation time is 0.85 decades at $T_g + 40$ K. We used this correction factor to deduce the relaxation time τ_n^{PI*} of PI in the media which has the same friction coefficient as that of PVE. Comparison of this relaxation time with τ_s^{PVE} yields the M_{PI} of the same size as the PVE segment. The τ_n^{PI*} and its extrapolation to τ_s^{PVE} are also shown in Figure 9. The result was $M_{PI} = 4.5 \times 10^2$ g mol^{-1}, and the corresponding length referred to as r_{medium} becomes 1.8 nm. This length can be regarded as the segment size of PVE. In addition, r_{long} (3 nm) should be the upper bound of the relevant length for the segmental motion in PI/PVE 75/25 blend. These three length scales determined here are schematically shown in Figure 10. The assumption we used here is that the *size* of the segmental unit can be substituted for several factors determined by the intrachain interactions such as the potential barrier for the internal rotation.

From the experimental uncertainties included in all the relaxation times, we estimated the error for these lengths as $r_{short} = 0.9 \pm 0.06$ nm, $r_{medium} = 1.8 \pm 0.3$ nm, and $r_{long} = 3.0 \pm 0.18$ nm. The largest error in r_{medium} is due to the uncertainty in the friction factor that was used to determine τ_n^{PI*}.

Temperature variation of these length scales is very important and desired information. However our analysis could not resolve this variation because we approximately regarded the T dependences of τ_n^{PI} and τ_s^{PI} to be the same. This approximation results in the T-independent length scale. We think that more precise dielectric measurements over wide frequency range for this blend system will probably resolve it in the future.

VI. Validity of the Two Length Scale Model. Several models utilizing the cooperative volume concept assume that a single length scale governs the segmental motions of the both components. (Kumar's theory took into account the distribution of the volume size but the distribution is unimodal). On the other hand the Lodge and McLeish model assumes two different sizes corresponding to the component Kuhn lengths (l_K) are relevant to the component dynamics. The assumptions of these models are also schematically shown in Figure

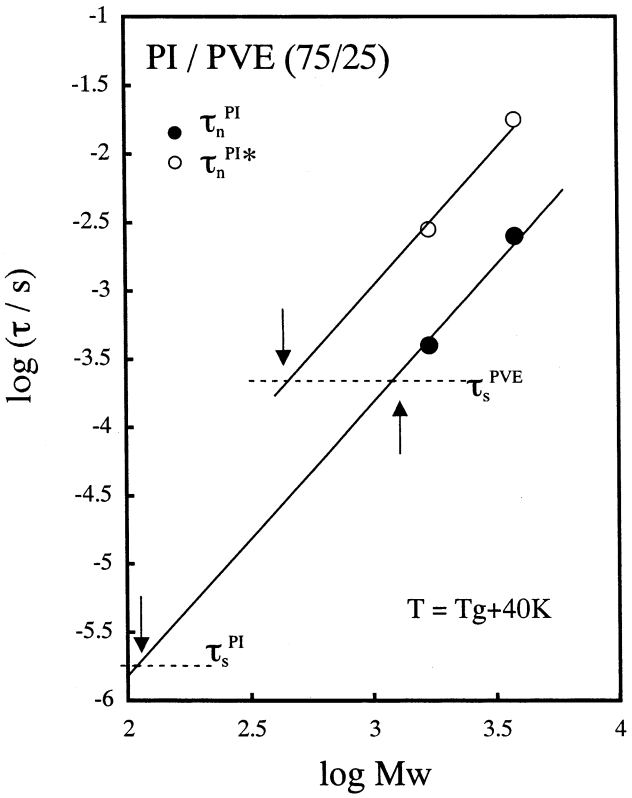

Figure 9. Molecular weight dependence of the normal mode relaxation time τ_n^{PI} in the blend of PI/PVE-602 (75/25) at $T = T_g + 40$ K. τ_n^{PI*} stands for the corrected relaxation time of PI to have the same friction factor with that of PVE segment. Here τ_s^{PVE} and τ_s^{PI} represent the segmental relaxation times of PVE and PI in the blend, respectively. The arrows indicate the determined molecular weights of PI which were converted to the three lengths, r_{short}, r_{long}, and r_{long}.

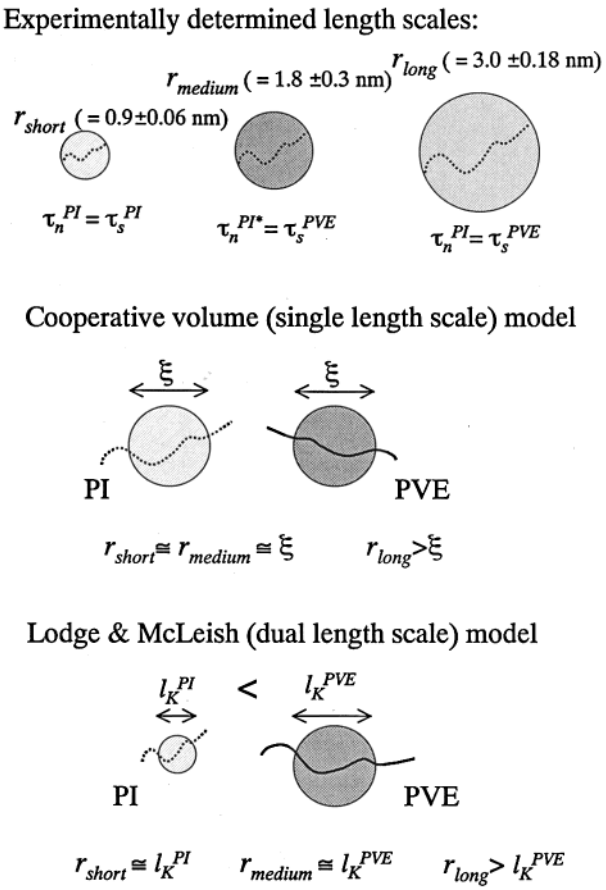

Figure 10. Schematic representation of the meaning of the determined length scales, r_{short}, r_{medium}, and r_{long}. The required relations for these length scales are also shown based on the cooperative volume model and Lodge and McLeish model.

10. In the single-sized cooperative volume model, r_{short} and r_{medium} should be the same, and these lengths correspond to the cooperative volume size (ξ). From the experimental result we can conclude that the single cooperative volume idea is invalid for PI/PVE blend. In addition, as for the cooperative length ξ, Kumar's model specifically predicts ξ as long as 8.6 nm for PI/PVE 75/25 blend at $T = T_g + 40$ K. (Here we used the parameters written in ref 23 to calculate ξ.) This value is much larger than r_{long} which is the upper bound of the segment size. This discrepancy indicates the inadequacy of the single length scale model. Although the absolute values of both r_{short} (0.9 ± 0.04 nm) and r_{medium} (1.8 ± 0.3 nm) are slightly larger than the reported Kuhn lengths (0.68 nm for PI and 1.16 nm for PVE, respectively), the ratio of these two lengths is nearly the same as that of Kuhn lengths within 15%. Therefore, our result strongly supports the view in Lodge and McLeish model that two length scales approximately corresponding to the Kuhn lengths coexist in the segmental motion of miscible blends. As for the reasons why the determined lengths are slightly larger than the Kuhn sizes, several possibilities can be considered such that the interchain cooperative motion and/or the difference between free chain ends (for end-to-end vector fluctuation) and fixed ends (for segmental motion) might play a role.

There remain some uncertainties in the manner of the extrapolation made in Figure 9. As described in the previous section, Rouse dynamics and Gaussian chain approximation are not validated for such low MW regions although these relations will probably hold in the MW region above the Kuhn unit. Therefore, we consider the limiting case that the PI chain behaves as a rigid rod. In that case, $\tau \propto M^3$ and $\langle r^2 \rangle \propto M^2$ and thus $\tau \propto r^3$. If these relations are applied to the PI chains with M_w below 10^3, the corresponding length scale decreases to be $r_{short} = 0.6 \pm 0.04$ nm and $r_{medium} = 1.6 \pm 0.3$ nm. This estimation will give the minimum values for these lengths. It is noteworthy to mention that the ratio of r_{medium}/r_{short} increases to $(r_{medium}/r_{short})^{4/3}$ in this estimation. Therefore, the picture for the coexistence of two different length scales is more conceivable.

In the previous section, we determined the length scale of PI to be 1.2 nm using the T_g^{eff} data. Then the lengths of the segments for PI and PVE became comparable. It contradicts the result obtained in this section. Concerning this contradiction, we think that the Lodge and McLeish model contains a fault in predicting the dynamics for the component of the smaller size and lower T_g in the blend. One of their assumptions is the transformability between ϕ_{eff} and T_g^{eff} for both components. In other words, this forces the assumption that the concentration (ϕ_{eff}) in the unit volume of l_K^3 is uniform and the segmental dynamics are simply governed by the friction factor determined by ϕ_{eff}. This may be valid for the PVE segment because l_K^{PVE} is larger than l_K^{PI} and the PI segment moves faster than PVE approximately leading to the simple dynamics of PVE segment determined by only ϕ_{eff} due to the time and spatial averaging effect inside the volume. However this will not be the case for the motion of PI segment. Since

the PVE component incorporated inside the volume of $(l_K^{PI})^3$ moves much slower than the PI segment, the concept of the uniform effective concentration (mean field approximation) is hardly acceptable. Probably a more detailed picture for such segmental motions, i.e., the mechanism of how the different kind of segments cooperatively move in the small volume, should be necessarily taken into account. Two pictures, for example, are considered here: (1) the PI segment cannot move until the motion for the portion of the PVE segment complete inside the volume of $(l_K^{PI})^3$, and (2) decoupling of the segmental motion of PI from that of PVE will take place. If the former is the proper picture for the PI/PVE blend, the T_g^{eff} of PI will become somewhat closer to the average T_g as observed in Figure 7.

Conclusion

The observed normal modes of PI in the blend with PVE were thermorheologically simple. Large size motions such as the normal mode will smear the inhomogeneity of the concentration due to the fluctuation effect.

As for the α-relaxations, tTS broke down especially in the frequency region between normal mode peak and segmental mode of PVE. As one of the reasons, we considered that it was due to the different T dependences of the normal mode of PI and the segmental mode of PVE. This was mainly the reason for the tTS break down observed in PVE 25% blend. On the other hand, for the blend of PVE 75% another factor (probably the composition fluctuation) was found to contribute to the broadening of the ϵ'' shape.

We determined the effective glass transition temperatures of both PI and PVE components from the shift factor data corresponding to the normal mode of PI and the segmental mode of PVE. Our result agreed fairly well with the NMR result obtained by Chung et al.[19]

From the comparison of the normal mode relaxation time and the segmental mode relaxation times, we experimentally determined three length scales r_{short}, r_{medium}, and r_{long} in PI/PVE 75/25 blend at $T = T_g + 40$ K. The result was that $r_{short} = 0.9 \pm 0.06$ nm, $r_{medium} = 1.8 \pm 0.3$ nm, and $r_{long} = 3.0 \pm 0.18$ nm. r_{short} and r_{medium} correspond to the sizes of the motional unit for the segmental relaxation of PI and PVE, respectively, and r_{long} is considered to be the upper bound for these sizes. These results proved the existence of two different length scales relevant to the segmental motion of each component in the blend and support the assumption made in the Lodge and McLeish model.

Acknowledgment. We acknowledge the financial support from the Ministry of Education, Culture, Sports, Science and Technology, Japan, under Grant-in-aid #13650955.

References and Notes

(1) Utracki, L. A. *Polymer alloys and Blends: Thermodynamics and Rheology*; Carl Hanser Verlag: Munich, Germany, 1989.
(2) Colby, R. H. *Polymer* **1989**, *30*, 1275.
(3) Roovers, J.; Toporowski, P. M.*Macromolecules* **1992**, *25*, 1096−1102.
(4) Roovers, J.; Toporowski, P. M.*Macromolecules* **1992**, *25*, 3454−3461.
(5) Pathak, J. A.; Colby, R. H.; Floudas, G.; Jerome, R. *Macromolecules* **1999**, *32*, 2553−2561.
(6) Alegria, A.; Colmenero, J.; Ngai, K. L.; Roland, C. M. *Macromolecules* **1994**, *27*, 4486-4492.
(7) Alvarez, F.; Alegria, A.; Colmenero, J. *Macromolecules* **1997**, *30*, 597−604.
(8) Arbe, A.; Alegria, A.; Colmenero, J.; Hoffmann, S.; Willner, L.; Richter, D. *Macromolecules* **1999**, *32*, 7572−7581.
(9) Roland, C. M.; Ngai, K. L. *Macromolecules* **1991**, *24*, 2261−2265.
(10) Roland, C. M.; Ngai, K. L. *Macromolecules* **1992**, *25*, 363−367.
(11) Ngai, K. L.; Roland, C. M.; O'Reilly, J. M.; Sedita, J. S. *Macromolecules* **1992**, *25*, 3906−3909.
(12) Cendoya, I.; Alegria, A.; Alberdi, J. M.; Colmenero, J.; Grimm, H.; Richter, D.; Frick, B. *Macromolecules* **1999**, *32*, 4065−4078.
(13) Zetsche, A.; Fischer, E. W. *Acta Polym.* **1994**, *45*, 168−175.
(14) Kanatakis, J.; Fytas, G.; Hadjichristidis, N. *Macromolecules* **1991**, *24*, 1806−1812.
(15) Kanatakis, J.; Fytas, G.; Kremer, F.; Pakula, T. *Macromolecules* **1992**, *25*, 3484−3491.
(16) Miller, J. B.; McGrath, K. J.; Roland, C. M.; Trask, C. A.; Garroway, A. N. *Macromolecules* **1990**, *23*, 4543−4547.
(17) Chin, Y. H.; Zhang, C.; Wang, P.; Inglefield, P. T.; Jones, A. A.; Kambour, R. P.; Bendler, J. T.; White, D. M. *Macromolecules* **1992**, *25*, 3031−3038.
(18) Chung, G.-C.; Kornfield, J. A.; Smith, S. D. *Macromolecules* **1994**, *27*, 964−973.
(19) Chung, G.-C.; Kornfield, J. A.; Smith, S. D. *Macromolecules* **1994**, *27*, 5729−5741.
(20) Min, B.; Qiu, X. H.; Ediger, M. D.; Pitsikalis, M.; Hadjichristidis, N. *Macromolecules* **2001**, *34*, 4466−4475.
(21) Lutz, T. R.; He, Y.; Ediger, M. D.; Cao, H.; Lin, G.; Jones, A. A. Submitted to *Macromolecules*.
(22) Arendt, B. H.; Krishnamoorti, R.; Kornfield, J. A.; Smith, S. D. *Macromolecules* **1997**, *30*, 1127−1137.
(23) Kamath, S.; Colby, R. H.; Kumar, S. K.; Karatasos, K.; Floudas, G.; Fytas, G.; Roovers, J. E. L. *J. Chem. Phys.* **1999**, *111*, 6121−6128.
(24) Hoffmann, S.; Willner, L.; Richter, D.; Arbe, A. Colmenero, J.; Farago, F. *Phys. Rev. Lett.* **2000**, *85*, 772−775.
(25) Arendt, B. H.; Krishnamoorti, R.; Kannan, R. M.; Seitz, K.; Kornfield, J. A.; Roovers, J. *Macromolecules* **1997**, *30*, 1138−1145.
(26) Katana, G.; Fischer, E. W.; Hack, Th.; Abetz, V.; Kremer, F. *Macromolecules* **1995**, *28*, 2714−2722.
(27) Milhaupt, J. M.; Lodge, T. P.; Smith, S. D.; Hamersky, M. W. *Macromolecules* **2001**, *34*, 5561−5570.
(28) Urakawa, O.; Fuse, Y.; Hori, H.; Tran-Cong, Q.; Yano, O. *Polymer* **2001**, *42*, 765−773.
(29) Roland, C. M. *Macromolecules* **1987**, *20*, 2557.
(30) Roland, C. M. *J. Polym. Sci., Polym. Phys. Ed.* **1988**, *26*, 839.
(31) Tomlin, D. W.; Roland, C. M. *Macromolecules* **1992**, *25*, 2994−2996.
(32) Kumar, S. K.; Colby, R. H.; Anastasiadis, S. H.; Fytas, G. *J. Chem. Phys.* **1996**, *105*, 3777−3788.
(33) Lodge, T. P.; McLeish, T. C. B. *Macromolecules* **2000**, *33*, 5278−5284.
(34) Donth, E. *J. Non Cryst. Solids* **1982**, *53*, 325−330.
(35) Adam, G.; Gibbs, J. H. *J. Chem. Phys.* **1965**, *43*, 139−146.
(36) Adachi, K.; Kotaka, T. *Prog. Polym. Sci.* **1993**, *18*, 585−622.
(37) Halasa, A. F.; Lohr, D. F.; Hall, J. E. *J. Polym. Sci., Polym. Chem. Ed.* **1981**, *19*, 1357−1360.
(38) Fox, T. G. *Bull. Am. Phys. Soc.* **1956**, *1*, 123.
(39) Gordon, M.; Taylor, J. S. *J. Appl. Chem.* **1952**, *2*, 495.
(40) Kwei, T. K. *J. Polym. Sci., Polym. Lett. Edn.* **1984**, *22*, 307.
(41) See, for example: Ferry, J. D. *Viscoelastic Properties of Polymers*; Wiley: New York, 1980.
(42) Adachi, K.; Hirano, H. *Macromolecules* **1998**, *31*, 3958−3962.
(43) Schonhals, A. In *Dielectric Spectroscopy of Polymeric Materials*; Runt, J. P., Fitzgerald, J. J., Eds.; American Chemical Society: Washington, DC, 1997; Chapter 3.
(44) We found that the difference in T_g^{eff}'s for the normal mode and segmental mode relaxation times of pure PI (by using the data in ref 43) were resolved to be less than 2 K.
(45) Adachi, K.; Nishi, I.; Itoh, S.; Kotaka, T. *Macromolecules* **1990**, *23*, 2550.

MA0217940